



Full Length Article

Combined application of electrical resistivity and GIS for groundwater exploration and subsurface mapping at northeast Qattara Depression, Western Desert, Egypt



M.I.I. Mohamaden ^a, H.M. El-Sayed ^{a,*}, S.A. Mansour ^b

^a National Institute of Oceanography and Fisheries, Alexandria, Egypt

^b Egyptian General Mineral Resources Authority, Egypt

ARTICLE INFO

Article history:

Received 29 August 2016

Received in revised form 26 October 2016

Accepted 27 October 2016

Available online 25 November 2016

Keywords:

Qattara Depression

Moghra Formation

Qatrani Formation

VES

ABSTRACT

The study area is located at northeast of Qattara Depression, Western Desert, Egypt. Geoelectrical resistivity method has been used by measuring twelve vertical electrical soundings using Schlumberger configuration with AB/2 spacing ranging from 1.5 m to 500 m in order to investigate the shallow groundwater aquifer and to delineate the subsurface structures in this area. The results revealed that the subsurface section consists of three geoelectrical units. The first unit is composed of surface Quaternary wadi deposits with resistivity values ranging from 248 to 1378 Ohm.m, and thickness ranging from 5.9 to 34.6 m. The second geoelectrical unit is composed of sandstone of Moghra Formation (Lower Miocene) with depth ranges from 5.9 to 34.6 m and its resistivity values range from 23 to 188 Ohm.m. This unit represents the main aquifer in the study area. The third geoelectrical unit is composed of claystone of Qatrani Formation with depth ranging from 106 to 174.4 m and resistivity values range from 0.5 to 9 Ohm.m. It extends to the maximum depth of penetration at the central part of the study area.

Structurally, the study area is affected by two probable faults trending mainly in NW-SE direction with upthrown side towards the central part of the study area forming a horst structure.

© 2016 Mansoura University. Production and hosting by Elsevier B.V. This is an open access article under the CC BY-NC-ND license (<http://creativecommons.org/licenses/by-nc-nd/4.0/>).

1. Introduction

The northeastern part of Qattara Depression is one of the highly promising areas for future development. In such area, groundwater is the main source of water and needs further exploration studies. The main aims of the present study are to explore the shallow sandstone aquifer and evaluating the structural elements affecting the study area which lies between latitudes 30.289549°N and 30.330554°N and longitudes 28.975918°E and 29.028553°E representing an area of about 20.5056 km² (Fig. 1).

The study area is located in the dry belt of Egypt. It is characterized by warm and hot climate in winter and summer, respectively. The average temperature is ranging between 39 °C in summer and 23 °C in winter [1]. The rate of natural evaporation between 5.1 mm/day in December to 14 mm/day during June at an average annual rate of 9.6 mm/day [1]. This area is suffering from a scarcity of rainfall; the annual precipitation ranges between 25 and 50 mm [2].

The electrical resistivity method is an effective geophysical tool which is widely used for groundwater exploration. It provides information about the subsurface structures and lithology [3]. The vertical electrical sounding (VES) method is used to provide reliable information about the shallow subsurface layers.

Many authors used the geoelectrical tool for investigating groundwater such as [3–10]. The main aims of the present study are to explore the sandstone aquifer and evaluating the structural elements affecting the study area.

2. Geologic setting

The study area is characterized by relatively low elevation (Fig. 2). The main surface geology was described in the geological map of Qattara Depression with scale 1:500,000 (Fig. 3). According to different studies on this area [11,12], the study area is covered by wadi and alluvial deposits of Quaternary age.

The northern border of the Qattara Depression is marked by a steep escarpment (250 m a.s.l.) of white limestone of the Middle Miocene Marmarica Formation. The Qattara Depression is cut into nearly horizontal beds of Miocene to Eocene age. The subsurface

* Corresponding author.

E-mail address: geo_hossam@yahoo.com (H.M. El-Sayed).

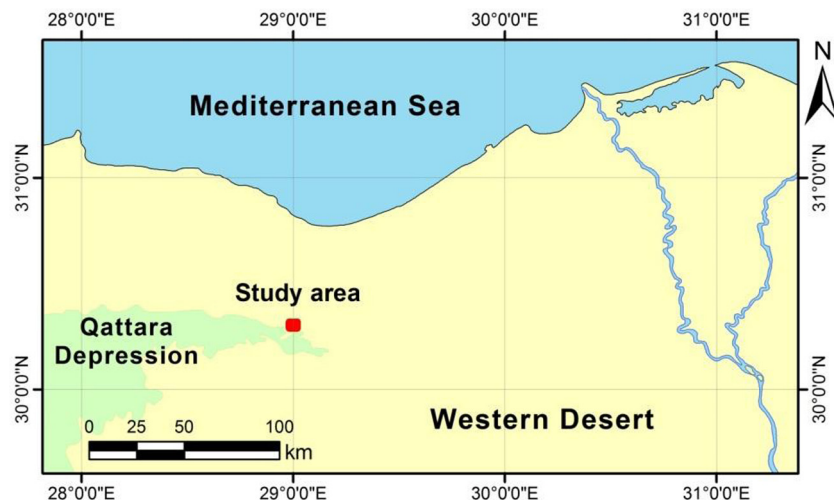


Fig. 1. Location map showing the study area.

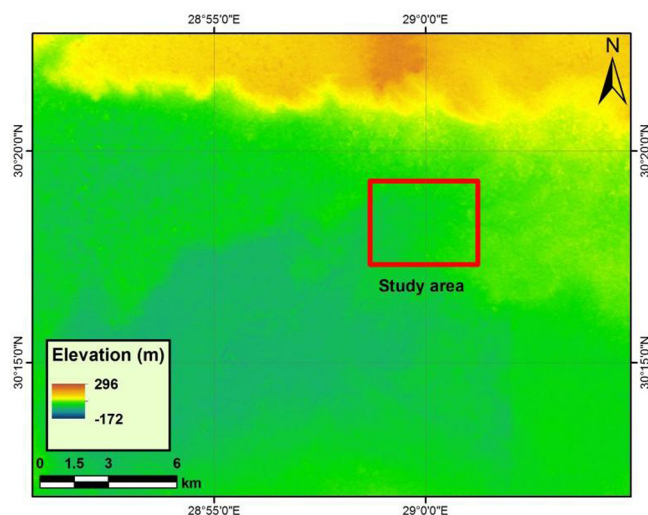


Fig. 2. Digital elevation model of Qattara Depression.

stratigraphy of the study area (Fig. 4) was described as follows [11,14]:

Quaternary Deposits: It consists of sand and dunes, especially at the southern part. **Lower Miocene Sediments:** It is represented by Moghra Formation which consists of white sand, sandstone, intercalated with shale and contains fossils of backbone, fossilized wood. It is considered as the shallow groundwater aquifer in this area. **Lower Oligocene Deposits:** It is represented by Qattrani Formation which is composed of sand, gravel and sandstone with overlaps of the shale. **Upper Eocene Deposits:** It is represented by Qasr El-Sagha and Birket Qarun Formations. It consists of sandstone, limestone and shale overlaying the surface of unconformity followed by sandstone and limestone and shale. **The East Middle Eocene sediments:** It is represented by Moqattam Formation which is a sequence of limestone and sandy limestone.

Upper Cretaceous: It is composed of the Nubian Sandstone which is mainly of sandstone. **Precambrian rocks:** It is represented by the igneous and metamorphic rocks.

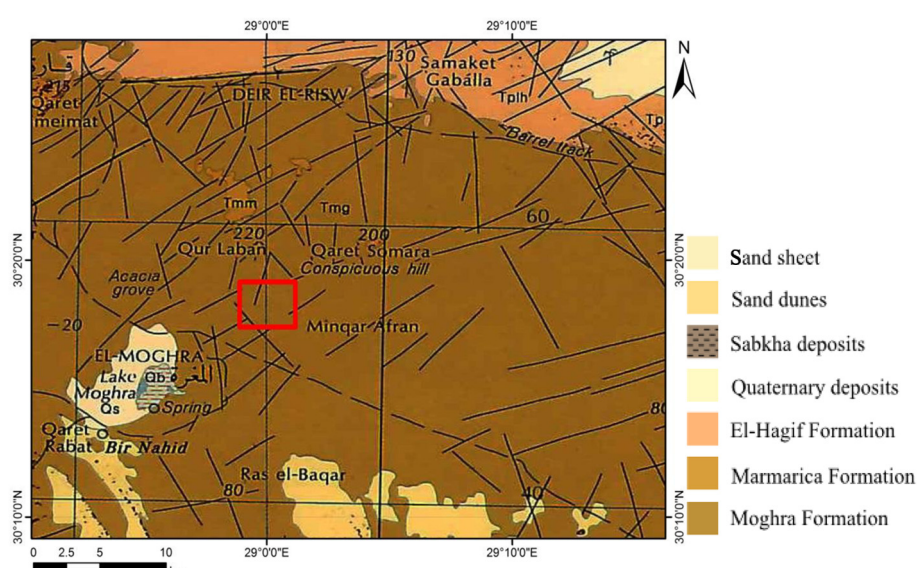


Fig. 3. Geological map of the study area (modified after Conoco, 1987) [13].

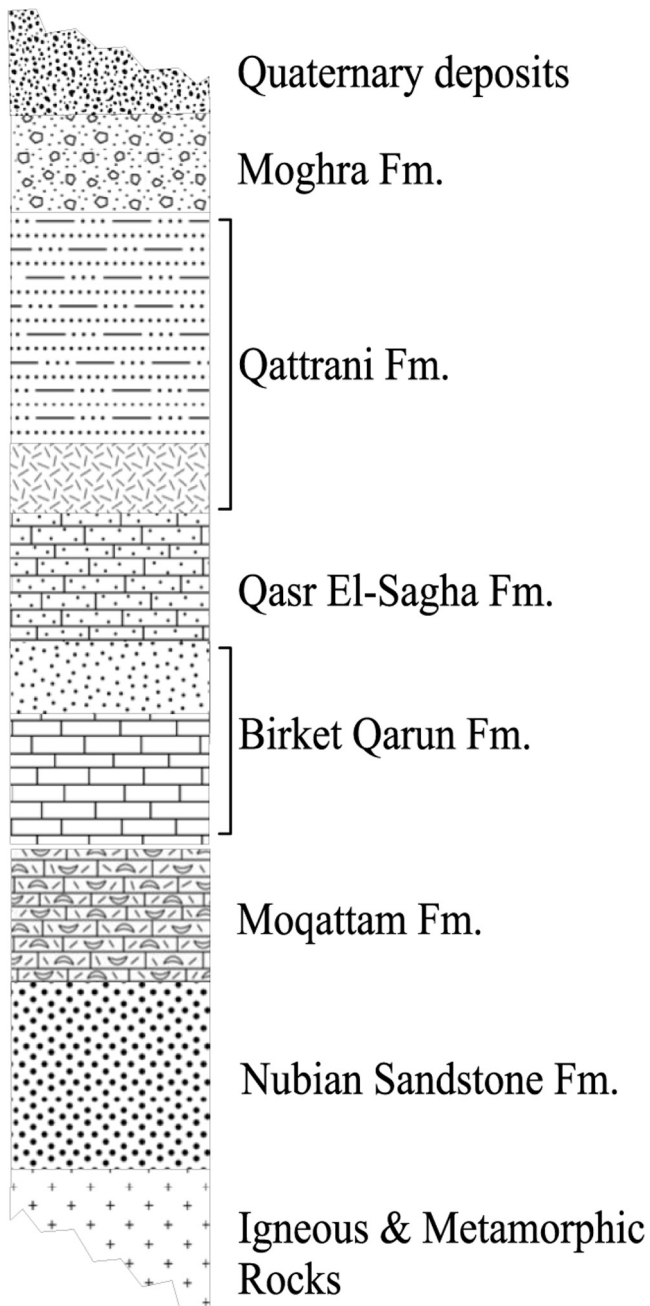


Fig. 4. Geological column of the study area (modified after Said, 1981) [11].

3. Materials and methods

3.1. Geoelectrical data

In this study, Syscal-Pro instrument was used in 2013 for measuring twelve vertical electrical soundings (VES's) using the Schlumberger configuration with total current electrode spacing ranging from 3 to 1000 m. The main objective is to detect the upper sandstone aquifer (Moghra Formation) and the structures affected the study area (Fig. 5).

In order to determine the subsurface layer parameters (resistivity and thickness), the manual interpretation technique was utilized by matching the plotted field curves with two layers master curves and the generalized Cagniard graphs [15,16]. The obtained results were introduced to the IPI2WIN software [17] as initial models to compute the final models (Fig. 6).

3.2. Geographic information system

Geographic information system (GIS) is a powerful tool that can help to overlay maps with different thematic data and facilitate map integration and analysis [18].

It was used to build a geodatabase containing the study area and the field measurements in order to generate contour maps showing the spatial variation of the measured apparent resistivity values and the groundwater depth in the study area.

The obtained data have been analyzed using the geostatistical analyst tools in ArcGIS software by examining the data using the exploratory spatial data analysis (ESDA) which is a set of tools that allow graphically exploring the data distribution, looking for outliers, looking for global trends and examining the spatial autocorrelation [19,20]. Each parameter of the measured data was examined by ESDA tools such as histogram and QQPlot to determine whether it is normally distributed or not and to determine the suitable type of data transformation if needed. The presence of global trends was also checked in each parameter using trend analysis tool which provides a three dimensional perspective of the data. The semivariogram tool was used to explore the spatial autocorrelation of the measured data [19].

Based on the ESDA data examination, the suitable interpolation method has been chosen for each parameter. Kriging method is one of the most common geostatistical interpolation methods. It is a probabilistic predictor which uses the least square linear regression algorithms to estimate the value of a continuous attribute in any unmeasured location using the values of the surrounding measured points [21–24]. The ordinary kriging method was used for interpolating the apparent resistivity values and the groundwater depth in the study area.

The digital elevation model (DEM) was used to extract the elevation value at the VES locations of the geophysical survey which is needed for constructing profiles. In this study, ASTER-GDEM-v.2 scene was analyzed using ArcGIS for this purpose.

4. Results and discussion

4.1. Iso-apparent maps

Iso-apparent maps (Fig. 7) shows that the surface layer is characterized by high resistivity values especially in the eastern parts which may be attributed to the surface unconsolidated quaternary deposits. Generally, the resistivity values tend to decrease in north-eastern parts due to the partial saturation of water. The spatial variation of the apparent resistivity values reflected that the study area may be affected by two faults at the central part with general tends of NW-SE directions.

4.2. Geoelectrical cross-sections

The results of VES's interpretation indicated that the number of layers in this area ranges between 2 and 3 layers.

4.2.1. Profile No. 1

This profile extends in the southeastern parts of the study area with a total length of about 3 km (Fig. 7a & b). It consists of four VES's named 1, 4, 7 and 10.

This cross-section shows that the subsurface section consists of three geoelectrical units. The first unit is composed of surface Quaternary wadi deposits with thickness ranging from 5.9 to 27 m and resistivity values ranging from 304 to 1333 Ohm.m. The second geoelectrical unit is composed of sandstone (Moghra Formation) with depth ranges from 5.9 to 27 m and its resistivity values range from 33 to 72 Ohm.m. This sandstone represents the main aquifer

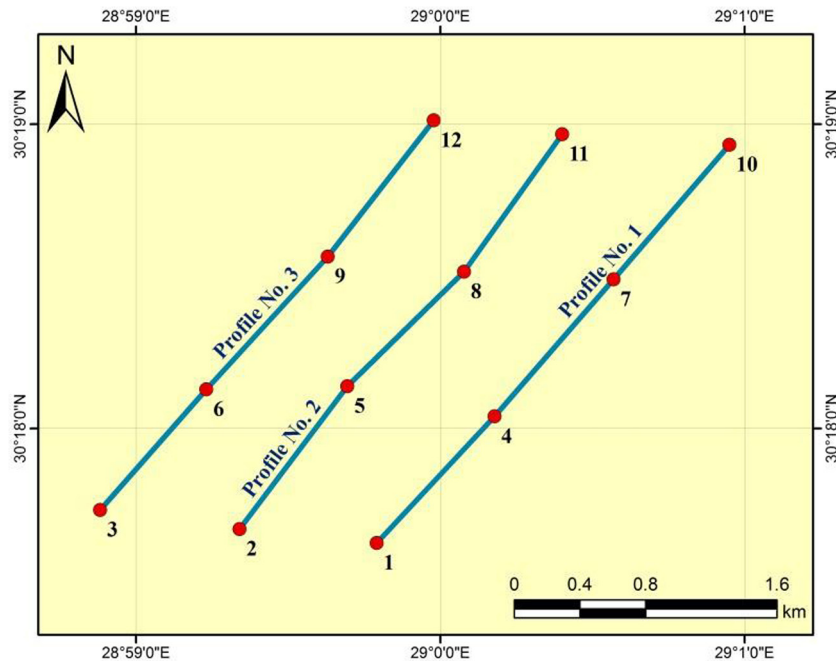


Fig. 5. Location map showing VES and profiles distribution.

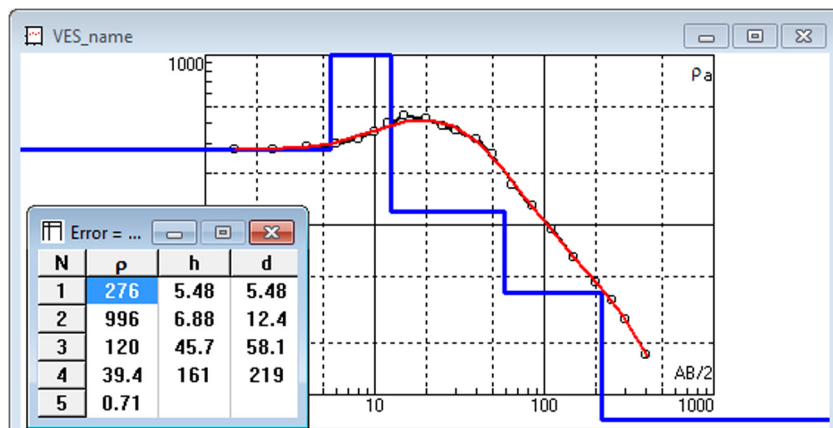


Fig. 6. Example of the layers model of VES No. 5.

in the study area. Moghra Formation extends to the maximum depth of penetration at the NE and SW part of this section (Fig. 8b), while at the central part of this section, the maximum depth ranges from 106 to 114.5 m. The Third geoelectrical unit is composed of claystone of Qattrani Formation with depth ranges from 106 to 114.5 m and its resistivity values range from 4 to 9 Ohm.m. This formation has been detected at the central part of this section. It extends to the maximum depth of penetration.

Structurally, this profile is affected by two probable faults. The first fault (F1) is located to the southwest of VES 10 with downthrown side towards the northeast, while the second fault (F2) is located to southwest of VES 4 with downthrown side towards the southwest. These two faults form a horst structure which reflects that the central part represents the shallower part of Moghra Formation (the main aquifer in the study area).

4.2.2. Profile No. 2

This profile extends in the central part of the study area with a total length of about 3 km (Fig. 9a & b). It consists of four VES's named 2, 5, 8 and 11.

The pseudo-section indicates that the central part of this section is affected by two faults. The geoelectrical cross-section shows that the subsurface section consists of surface Quaternary wadi deposits; its thickness ranges from 6.2 to 33.2 m and its resistivity values range from 410 to 1004 Ohm.m. The thickness of this unit increases from NE to SW direction; while the true resistivities increase at the central part of this section. The second geoelectrical unit is composed of Moghra Formation (the main aquifer) with depth ranging from 6.2 to 33.2 m and its resistivity values range from 70 to 188 Ohm.m. This unit extends to the maximum depth of penetration at the two sides of this section; while in the central part it extends to a depth ranging from 106.1 to 115.2 m. The Third

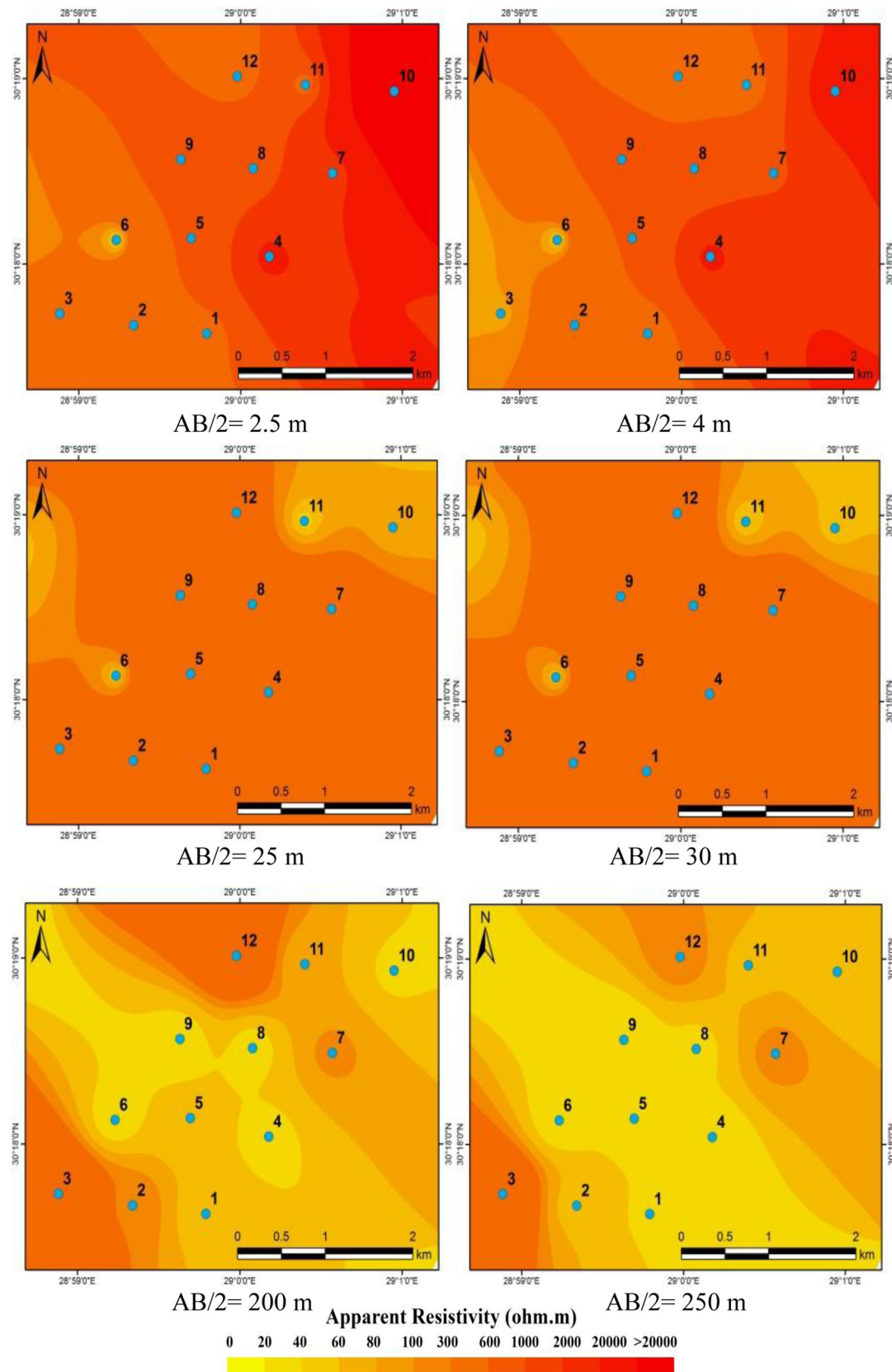


Fig. 7. Iso-apparent resistivity maps.

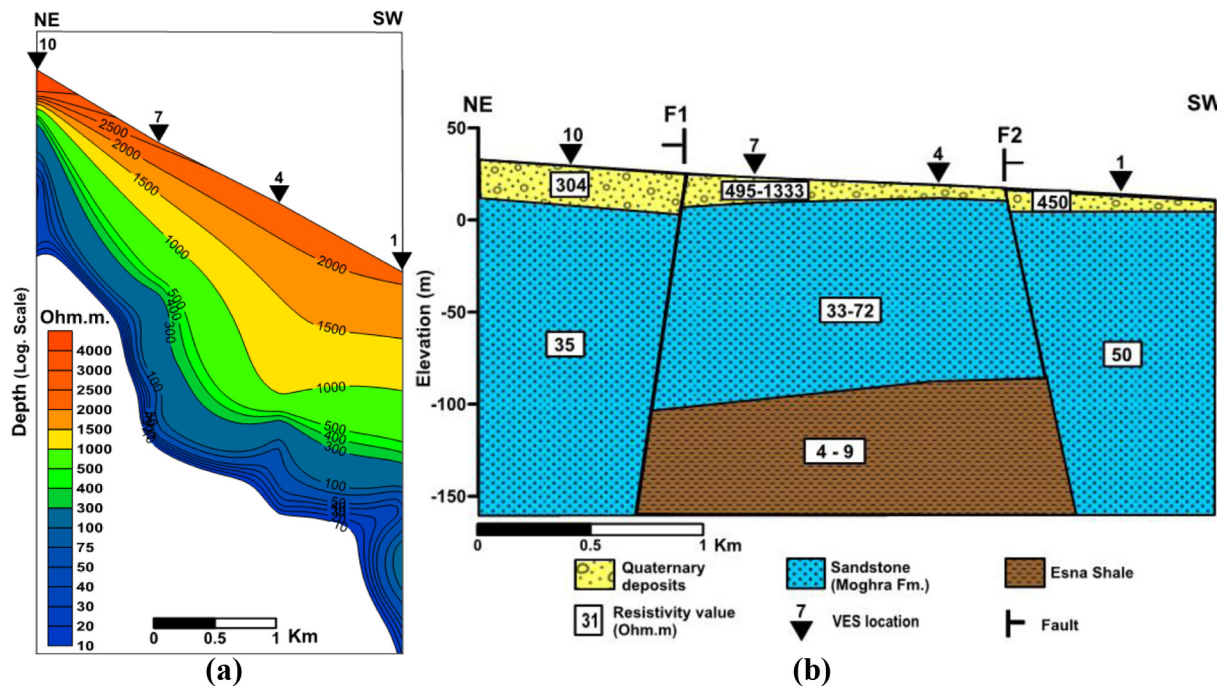


Fig. 8. Profile No. 1 (a) Pseudo-section (b) Geoelectrical cross-section.

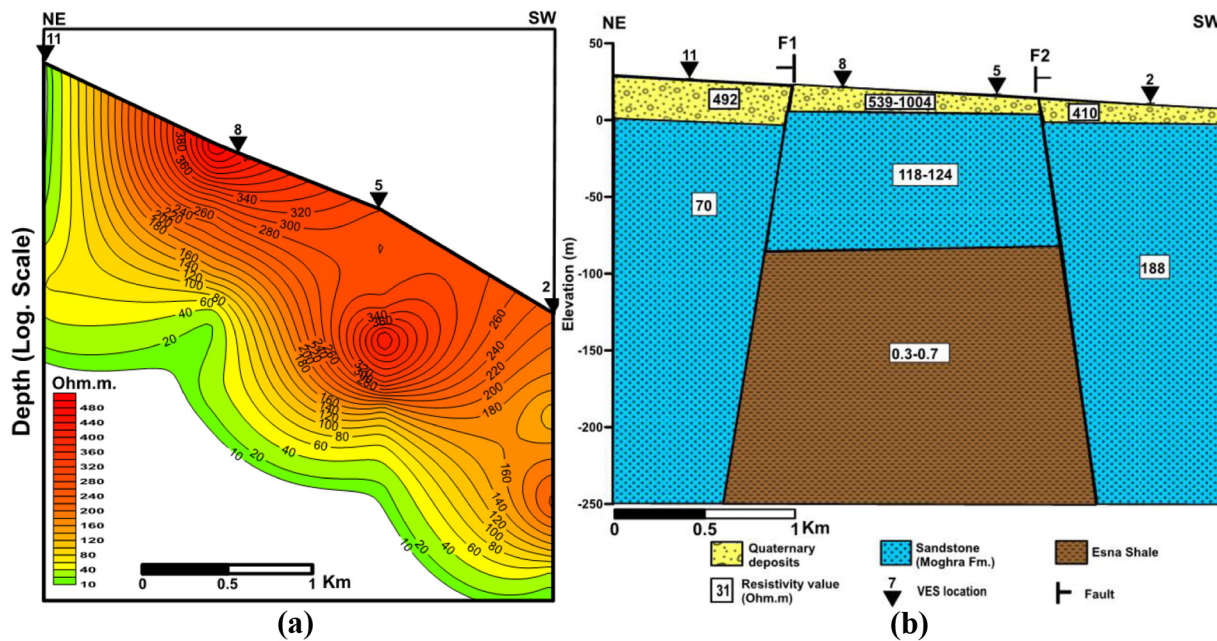


Fig. 9. Profile No. 2 (a) Pseudo-section (b) Geoelectrical cross-section.

geoelectrical unit is composed of claystone of Qatrani Formation with depth ranging from 106.1 to 115.2 m and its resistivity values range from 0.3 to 0.7 Ohm.m. This formation has been only detected at the central part of this profile.

Structurally, this profile is affected by two probable faults. The first fault (F1) is located to the southwest of VES 11 with down-thrown side towards the northeast, while the second fault (F2) is located to southwest of VES 5 with downthrown side towards the southwestern direction. These two faults form a horst structure.

4.2.3. Profile No. 3

This profile extends in the western parts of the study area with a total length of about 3 km (Fig. 10a & b). It consists of four VES's named 3, 6, 9 and 12.

The pseudo-section indicates that the central part of this section is affected by two faults. The geoelectrical cross-section shows that the subsurface section consists of surface Quaternary wadi deposits with thickness ranging from 7.2 to 34.6 m and its resistivity values range from 248 to 1378 Ohm.m. The thickness of this unit increases from NE to SW direction. The second geoelectrical unit

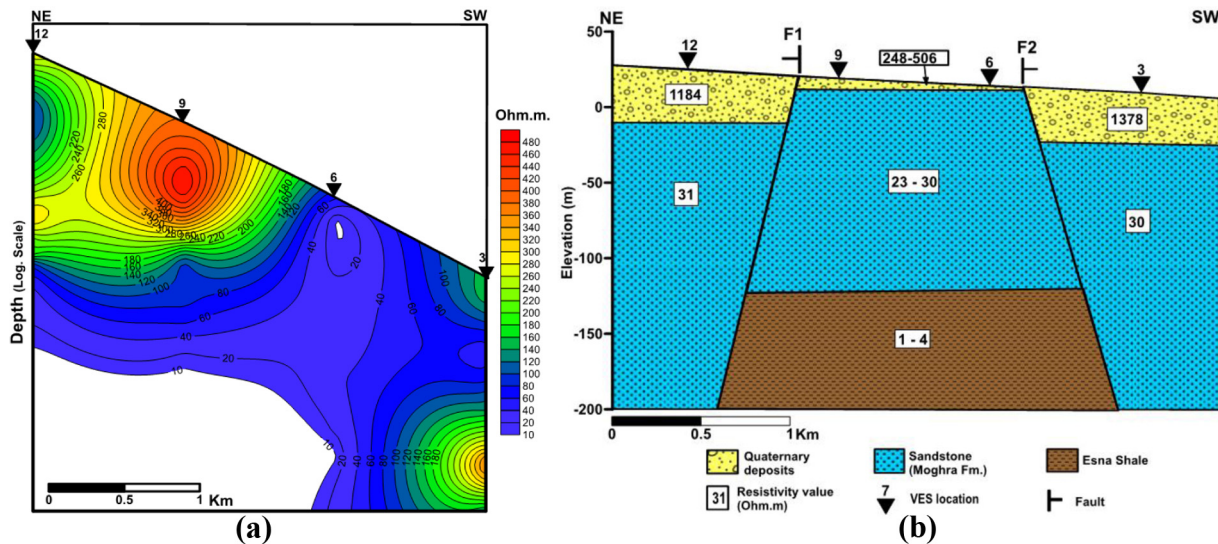


Fig. 10. Profile No. 3 (a) Pseudo-section (b) Geoelectrical cross-section.

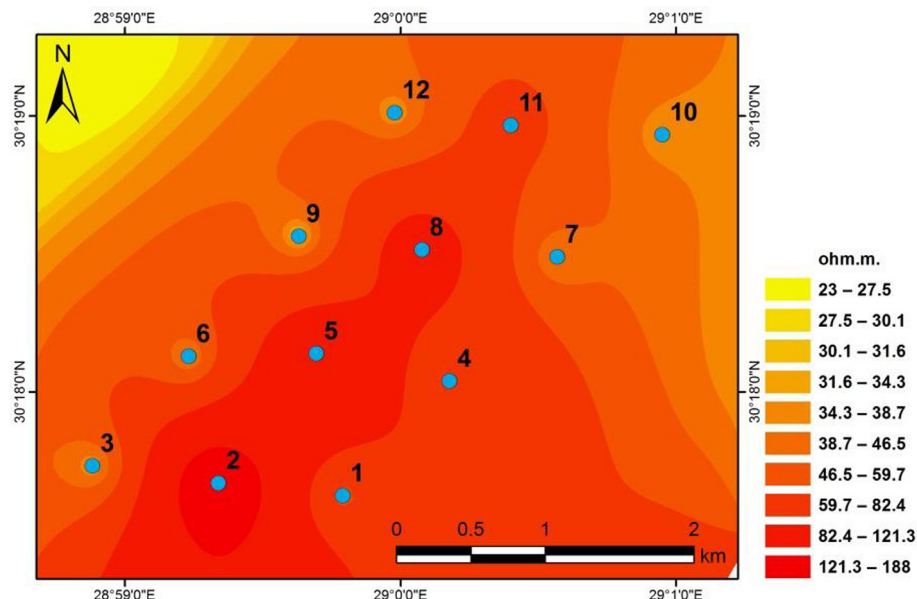


Fig. 11. True resistivity map of the water bearing layer.

is composed of Moghra Formation with depth ranging from 7.2 to 34.6 m and its resistivity values range from 23 to 31 Ohm.m. This unit extends to the maximum depth of penetration at the two sides of this section, while in the central part it extends to a depth ranging from 141.1 to 174.4 m. The Third geoelectrical unit is composed of claystone of Qattrani Formation with depth ranging from 141.4 to 174.4 m and its resistivity values range from 0.5 to 4 Ohm. m. This formation has been detected at the central part of this profile.

Structurally, this section is affected by two probable faults. The first fault (F1) is located to the southwest of VES 12 with downthrown side towards the northeastern direction, while the second fault (F2) is located to southwest of VES 6 with downthrown side towards the southwestern direction. These two faults form a horst structure.

The true resistivity of the water bearing layer (Moghra Formation) increases towards the central part of the study area (Fig. 11). The depth of groundwater decreases towards the western and southeastern parts, while it increases in the northeastern parts of the study area as shown in Fig. 12.

5. Conclusion

Twelve VES's have been carried out to provide reasonable results about the subsurface formations. Iso-apparent maps show that the surface layer is characterized by high resistivity values which may be attributed to the surface unconsolidated quaternary deposits. Generally, the resistivity values tend to decrease in the whole study area with depth as a result of the subsurface saturation.

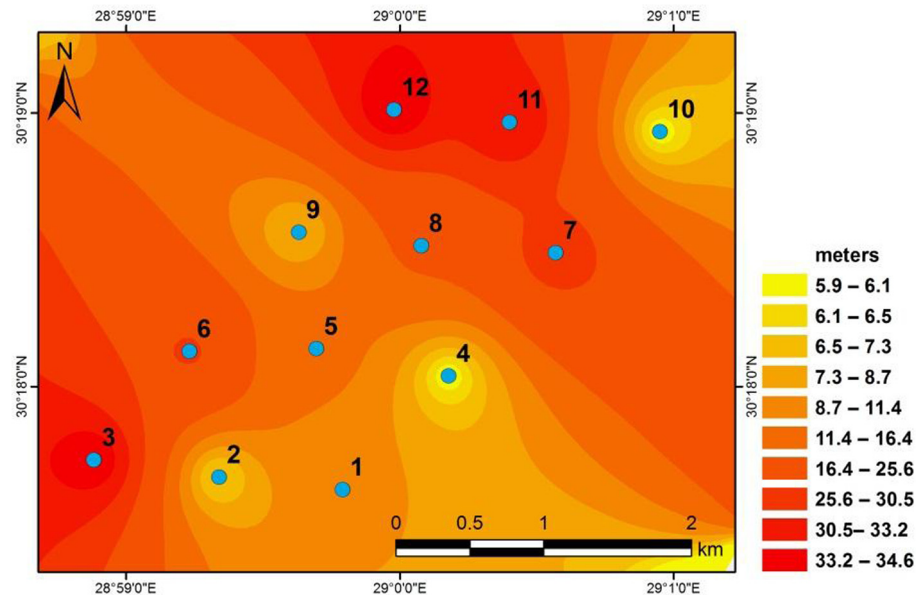


Fig. 12. Depth map of the groundwater (Moghra Formation).

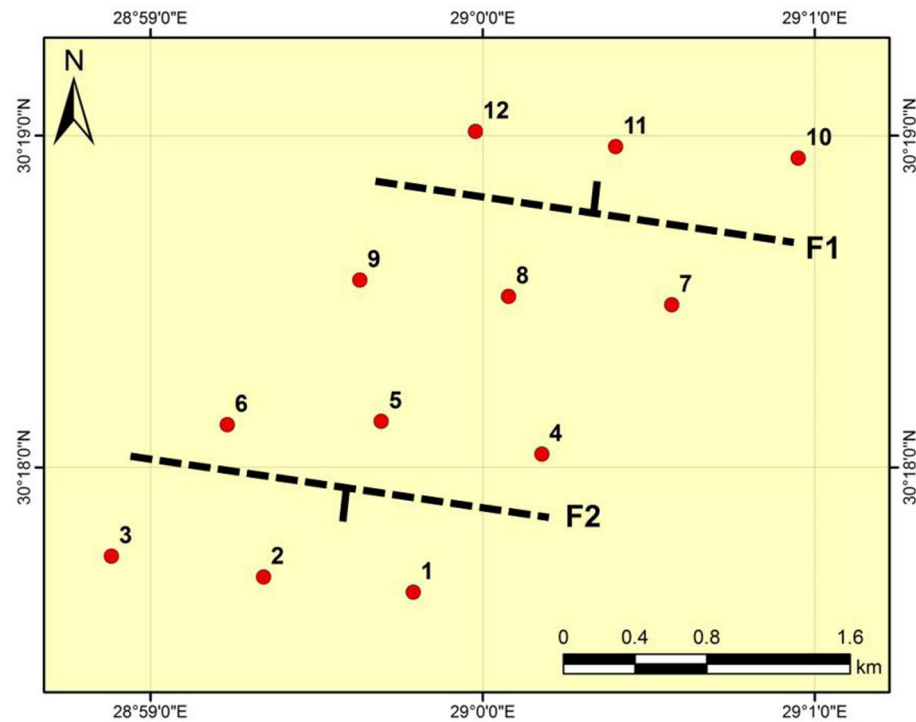


Fig. 13. Sketch map for faults directions.

tion with water. The central part of the study area is characterized by higher resistivity which may be attributed to the presence of Moghra Formation that represents the main aquifer in the study area. The results of VES's interpretations indicated that the number of layers in this area is ranging between 2 and 3 layers.

The first layer is composed of surface Quaternary wadi deposits with resistivity values ranging from 248 to 1378 Ohm.m. and a thickness ranging from 5.9 to 34.6 m. The second geoelectrical layer is composed of Moghra Formation (Lower Miocene) with depth ranges from 5.9 to 34.6 m and its resistivity values range

from 23 to 188 Ohm.m. This layer represents the main aquifer in the study area. The third geoelectrical layer is composed of claystone of Qatrani Formation with depth ranging from 106 to 174.4 m and resistivity values ranging from 0.5 to 9 Ohm.m.

Structurally, the study area is affected by two probable faults trending mainly in the NW-SE direction with upthrown side towards the central part of the study area forming a horst structure (Fig. 13).

Generally, the most promising area for drilling new wells is located at the extremely two ends of the NE-SW profiles.

References

- [1] Ezz El-Deen HMM, Abdallah AA, Barseim MSM. Geoelectrical study on the groundwater occurrence in the area southwest of Sidi Barrani, Northwestern Coast, Egypt. *Geophys Soc J* 2005;3:109–18.
- [2] Aref MAM, El-Khoriby E, Hamdan MA. The role of salt weathering in the origin of the Qattara Depression, Western Desert, Egypt. *Geomorphology* 2002;45:181–95.
- [3] Keller GV. Application of resistivity method in mineral and groundwater exploration Programs. *Geophys Surv Con* 1967;26:51–66.
- [4] Mohamaden MII. Electric resistivity investigation at Nuweiba Harbor of Aqaba, South Sinai, Egypt. *Egypt J Aqua Res* 2005;31:58–68.
- [5] Mohamaden MII. Groundwater exploration at Rafah, Sinai Peninsula, Egypt. *Egypt J Aqua Res* 2008;35:49–68.
- [6] Mohamaden MII, Abu Shagar S. Structural effect on the groundwater at the Arish City, North eastern Part of Sinai Peninsula, Egypt. *Egypt J Aqua Res* 2008;35:31–47.
- [7] Mohamaden MII, Abu Shagar S, Gamal AA. Geoelectrical survey for groundwater exploration at the Asyut Governorates, Nile Valley, Egypt. *J King Abdulaziz Univ Marine Sci* 2009;20:91–108.
- [8] Santos FAM, Sultan SA, Represas P, El Sorady AL. Joint inversion of gravity and geoelectrical data for groundwater and structural investigation: application to the northwestern part of Sinai, Egypt. *Geophys J Int* 2006;165:705–18.
- [9] Sultan AS, Mohamedien MII, Santos FAM. Hydrogeophysical study of the El Qaa Plain, Sinai, Egypt. *Bull Eng Geol Environ* 2009;68:525–53.
- [10] Mohamaden MII, Wahaballa A, El-Sayed HM. Application of electrical resistivity prospecting in waste water management: a case study Kharga Oasis, Egypt. *Egypt J Aqua Res* 2016;42:33–9.
- [11] Said R. The geological evaluation of the River Nile. New York: Springer-Verlag; 1981. p. 174.
- [12] Rizk ZS, Davis AD. Impact of the proposed Qattara Reservoir on the Moghra Aquifer of the Northwestern Egypt. *J Groundwater* 1991;29:232–8.
- [13] Conoco Coral. Geological map of Egypt, scale 1:500,000-NH 35 NE-Alexandria, Egypt. Cairo, Egypt: The Egyptian General Petroleum Corporation; 1987.
- [14] Khan SD, Fathy MS, Abdelaeme M. Remote sensing and geophysical investigations of Moghra Lake in the Qattara Depression, Western Desert, Egypt. *J Geomorphol* 2014;207:10–22.
- [15] Koefoed O. A generalized cagniard graph for interpretation of geoelectrical sounding data. *Geoph Prosp* 1960;8:459–69.
- [16] Orellana E, Mooney HM. Master table and curves for vertical electrical sounding data. *Geoph Prosp* 1966;8:459–69.
- [17] Bobatchev A, Modin I, Shevkin V. IPI2WIN V.2 for VES data interpretation. Russia: Dept. of Geophysics, Geological Faculty, Moscow State University; 2001.
- [18] Khalifa N, Abdel-Halim N. An evaluation of the GIS industry in Egypt. In: International conference on information technology and computer systems engineering ITCSE.
- [19] ESRI. Using ArcGIS geostatistical analyst. Redlands, CA, USA: Environmental Systems Research Institute; 2003.
- [20] El-Sayed HM. Hydrogeophysical and pedological investigations using GIS for land use planning of Barrani-Salum sector, Northwestern Coast, Egypt [Ph.D. thesis]. Egypt: Faculty of Science, Alexandria University; 2016. p. 52–7.
- [21] ESRI. ArcGIS geostatistical analyst. Redlands, CA, USA: Environmental Systems Research Institute; 2010.
- [22] Krivoruchko K. 2012. Empirical Bayesian kriging. ArcUser, Fall 2012. <<http://www.esri.com/news/arcuser/1012/empirical-bayesian-kriging.html>>.
- [23] Jensen JR, Jensen RR. Introductory geographic information systems. Toronto: Pearson; 2013.
- [24] ESRI, 2013. ArcGIS Desktop: Release 10.2. Environmental Systems Research Institute, Redlands, CA, USA.